Available online at www.sciencedirect.com
ScienceDirect
Ceramics International 37 (2011) 1563–1568
CERAMICS INTERNATIONAL
www.elsevier.com/locate/ceramint

An aqueous synthesis of photocatalyst by selective dissolution of titanium oxide/hydroxyapatite composite

Y. Ono [a,*], T. Rachi [a], T. Okuda [a], M. Yokouchi [a], Y. Kamimoto [a], H. Ono [a], A. Nakajima [b], K. Okada [c]

[a] Mechanical and Material Engineering Division, Kanagawa Industrial Technology Center, Ebina, Kanagawa 243-0435, Japan
[b] Department of Metallurgy and Ceramics Science, Tokyo Institute of Technology, Meguro, Tokyo 152-8552, Japan
[c] Materials and Structures Laboratory, Tokyo Institute of Technology, Midori, Yokohama 226-8503, Japan

Received 29 September 2010; received in revised form 10 October 2010; accepted 12 January 2011
Available online 18 February 2011

Abstract

A novel synthesis method of a highly active photocatalyst was proposed. Titanium dioxide (TiO_2) nano-particles were prepared by three-step procedure, precipitation of hydroxyapatite (HAp) on TiO_2 particles, heat treatment of the TiO_2/HAp composites, and acid treatment in hydrochloric acid. The unique point of this procedure is the selective dissolution of HAp to obtain exposed TiO_2 surfaces. The HAp precipitation was achieved by stirring TiO_2 powders in the mixtures of $Ca(NO_3)_2$ and $NH_4H_2PO_4$ aqueous solutions at pH 8.5. Then, the heat-treated TiO_2/HAp composites were treated with hydrochloric acid. The precipitated HAp avoided the direct contact of TiO_2 particles and suppressed the phase transformation from anatase-to-rutile >200 °C. The HAp also suppressed a decrease of specific surface area of TiO_2 during the heat treatment. The photocatalytic activities were evaluated from an absorbance decrease of methylene blue (MB) under ultraviolet (UV) irradiation. The MB photodecomposition was approximated to the first-order reaction and the reaction rate constants of the obtained TiO_2 powders heated at various temperatures were higher than those of conventional TiO_2 powders heated at same temperatures. The enhanced photocatalytic activity is attributed to the suppression effects for the phase transformation to rutile phase and the decreasing of specific surface area in the heat treatment.

Keywords: A. Grain growth; D. Apatite; D. TiO_2; Phase transition

1. Introduction

Titanium dioxide (TiO_2) is a well-known photocatalyst [1]. Many studies have been performed on the applications of TiO_2 photocatalyst to water and air purification because TiO_2 can photodecompose most organic matters by an electron excitation [2]. Electron and hole pairs are generated when TiO_2 is irradiated by ultraviolet (UV) light. The electron and hole produce radical species by a reduction or oxidation of adsorbed water. These radicals can decompose most organic matters [3]. To achieve a high photocatalytic activity, it is essential to suppress a recombination of electron–hole pairs [4,5]. This is generally achieved by high temperature calcination. However, an introduction of thermal energy induces particle agglomerations with a significant loss of specific surface area with phase transformation from anatase-to-rutile, which is generally considered to have lower photocatalytic activity than anatase [6]. It is, thus, difficult to enhance crystallinity of anatase suppressing decrease of the specific surface area and anatase phase ratio by the heating procedure.

Stabilizing anatase phase [7–11] is known as a successful procedure for the synthesis of highly active photocatalyst [12–15]. Park et al. [12] synthesized (Fe + Zn)/TiO_2 nano-particles by a flame aerosol method. This composite had higher photocatalytic activity than a pure TiO_2 powder in the degradation of 2-propanol. They explained that a critical factor in the photocatalytic activity is a high anatase phase ratio as well as high specific surface area and high crystallinity. The stabilization of anatase phase has also been achieved by adding oxides such as SiO_2 [9,10,14,15] and Al_2O_3 [11]. For example, Jung and Park [15] synthesized a silica-embedded TiO_2 by sol–gel method and reported that the embedding of silica into

* Corresponding author. Tel.: +81 46 236 1500; fax: +81 46 236 1525.
E-mail address: ono-y@kanagawa-iri.go.jp (Y. Ono).

0272-8842/$36.00
doi:10.1016/j.ceramint.2011.01.025

anatase matrix enhanced the thermal stability of TiO_2 nanoparticles resulting in the suppression of the phase transformation from anatase to rutile. The silica-embedded TiO_2 powder had higher photocatalytic activity than that of pure TiO_2 despite of a decrease of the exposed TiO_2 surface. They concluded that a heat treatment at high temperature without forming rutile is a key to the high photocatalytic activity due to the reduction of bulk defects, which are responsible for the low photocatalytic activity.

In the present study, anatase was stabilized by a precipitation of hydroxyapatite ($Ca_{10}(PO_4)_6(OH)_2$, HAp) on TiO_2 particle. The HAp precipitated TiO_2 composite particles [16–18] were prepared by changing of pH in the suspension. Then, they were heated at various temperatures and the resulting sample was treated in HCl solution to remove the HAp. The most different point from the previous studies is the additional procedure of the acid treatment to obtain an exposed TiO_2 surface. The resulting samples were characterized by various methods and evaluated their photocatalytic activity using methylene blue (MB) [19].

2. Experimental procedure

The commercial highly active TiO_2 powder (P25, supplied by Degussa Corporation) was used as the starting material. The experimental flow chart for sample preparation is shown in Fig. 1. The TiO_2 powder (0.5 mg) was ultrasonically dispersed in a solution (100 ml) dissolving $NH_4H_2PO_4$ (1.0 mg) and $Ca(NO_3)_2{\cdot}4H_2O$ (3.4 mg) adjusted the pH at 8.5 by 15 mass% NH_4OH solution and stirred for 3 days. All of these chemicals were purchased from Wako Pure Chemicals, Japan. The filtrated samples were dried at 110 °C for 24 h and heat-treated at 600–900 °C for 2 h. The resulting samples were treated in HCl solution (1 mol/l) for 1 h and centrifuged 6 times with distilled water to rinse the powder surface. The sample obtained at each synthesis step is designated as samples (a), (b), (c), and (d). For the reference, P25 powders were heat-treated at 500–900 °C for 2 h.

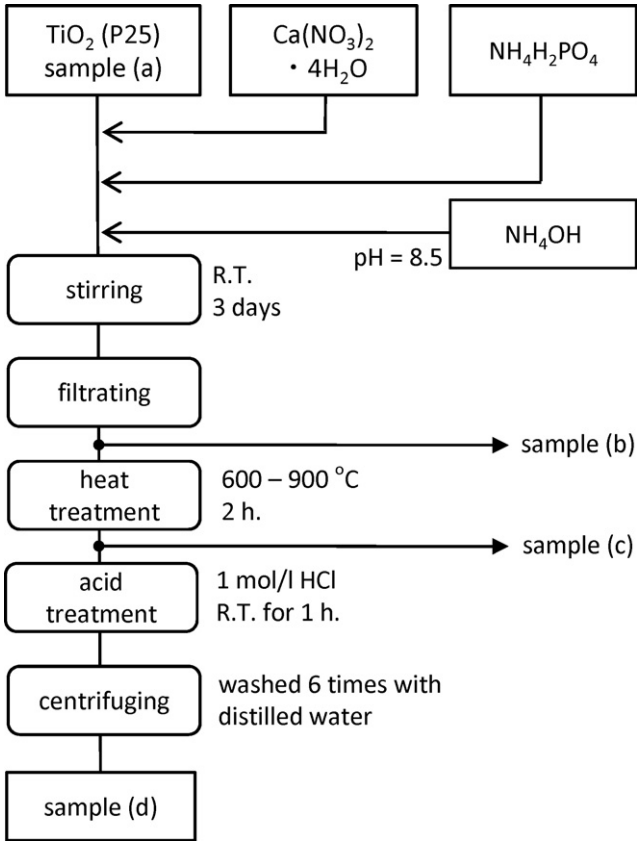

Fig. 1. Experimental flow scheme for the preparation of TiO_2 powder by three-step procedure.

The samples (a)–(d) were characterized by various methods. The XRD patterns were obtained using PHILIPS XPert diffractometer with a monochromated Cu Kα radiation. The mass ratio of rutile in the acid treated sample (d) was evaluated from the Spurr's equation [20]:

$$F_R = 1 - \frac{1}{1 + 1.26(I_R(110)/I_A(101))}, \quad (1)$$

where F_R is the mass ratio of rutile in the sample, $I_A(101)$ and $I_R(110)$ are the integrated 101 intensities of anatase and 110 of rutile, respectively. The SEM images were obtained using FE-SEM (FEI, SIRION) at an acceleration voltage of 15 kV. The specific surface area was calculated using Brauner–Emmett–Teller (BET) by a single-point method (CHEMBET-3000, YUASA) using nitrogen. The sample was dried at 150 °C for 24 h before the measurement.

The photocatalytic activity was evaluated from the decrease in the concentration of MB under UV (254 nm) irradiation [19]. The powder sample (10 mg) was dispersed ultrasonically for 10 min in 10 μM MB solution (50 ml) and stirred for 24 h in the dark. The resulting suspension was ultrasonically treated again for 10 min and irradiated UV at the intensity of 1.0 mW/cm^2. The absorbance at a wavelength of 664 nm was measured by a UV–vis spectrometer (UV-3100PC, SHIMADZU) to determine an MB concentration.

3. Results and discussion

3.1. Chemical reactions at each stage of the synthesis

In this study, TiO_2 nano-particles were prepared by the three-step procedure: (1) precipitation of HAp on TiO_2 surfaces in an aqueous solution, (2) heat treatment at 600–900 °C and (3) acid treatment in HCl solution (1 mol/l) to remove the surface HAp. Fig. 2 shows the XRD patterns obtained after each synthetic step (samples (b)–(d)) together with the starting material, P25. The P25 powder contained both anatase (as the major phase) and rutile (as the minor phase). The broad peaks assigned to HAp were detected in the sample (b), which was obtained after the precipitation of HAp. These peaks remained even after the heat treatment at 700 °C for 2 h with an increase of their crystallinity (sample (c)). Fig. 3 shows the XRD patterns of the TiO_2/HAp composites heated at various temperatures. The HAp began to decompose and $Ca_3(PO_4)_2$ (TCP) was formed above 850 °C. The XRD pattern of the sample (d) prepared by acid treatment of the TiO_2/HAp

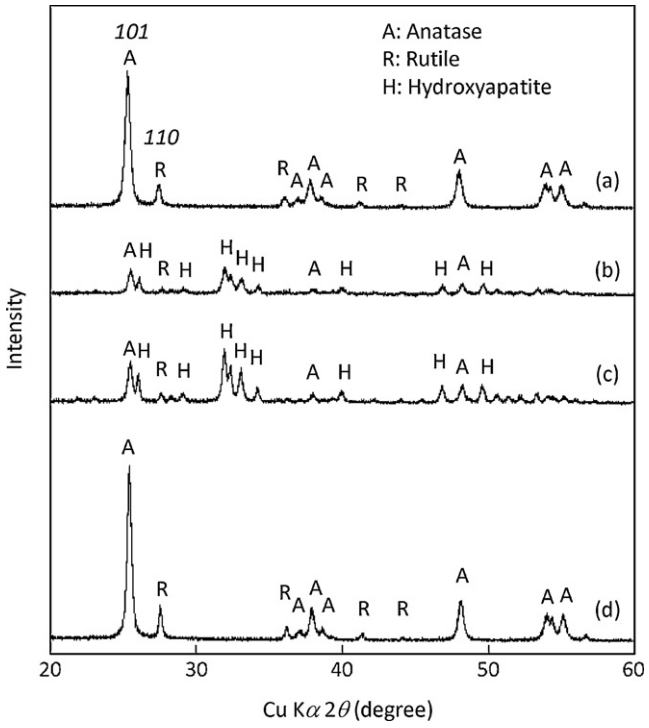

Fig. 2. XRD patterns obtained in a series of synthetic procedure, (a) starting material, (b) after precipitation, (c) after heat treatment at 700 °C, and (d) after acid treatment.

composite heated at 700 °C (Fig. 2(d)) showed disappearance of the HAp peaks and appearance of anatase and rutile peaks. Thus, acid treatment is thought to be successfully done under this condition. Fig. 4 shows the SEM images of samples (a)–(d).

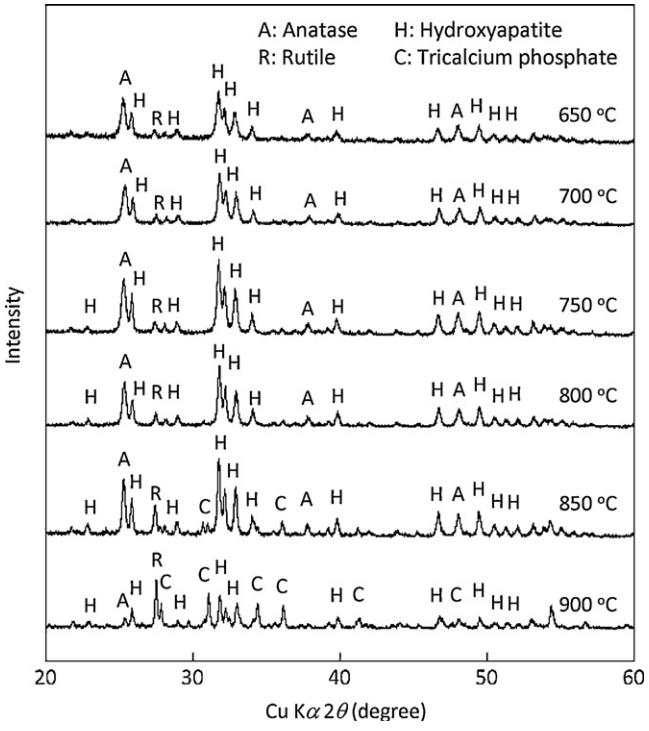

Fig. 3. XRD patterns obtained after heat treatment of TiO_2/HAp composites with various heating temperatures.

The particle size of the starting material, P25, was about 30 nm with a spherical shape. After the precipitation of HAp, elongated particles were observed in Fig. 4(b) and the particle size was smaller than 100 nm. After the heat treatment at 700 °C (Fig. 4(c)), the composite particles were found to agglomerate. After the acid treatment (Fig. 4(d)), the HAp seemed to be dissolved and the resulting particle size became almost same size with the starting P25.

3.2. Effect of HAp precipitation on phase transformation and specific surface area

The main objects of this study are to suppress the phase transformation and a decrease of specific surface area by the three-step method as HAp coating, heating and selective leaching of the HAp. The effect of the HAp precipitation on the anatase-stabilization was evaluated from a comparison of the phase transformation temperature from anatase to rutile. Fig. 5 shows changes of mass ratios of rutile in the present three-step and conventional one-step procedures as a function of heating temperature. In the one-step procedure, the starting material, P25, contains 17 mass% rutile. This sample started the anatase-to-rutile transformation by heating at 600 °C and saturated at 800 °C. By contrast, the phase transformation started by heating at 800 °C in the present three-step procedure, being about 200 °C shifted by the HAp precipitation. Comparing the phase transformation temperature with the decomposition temperature of HAp, both reactions were found to occur at almost same temperature, at 800–850 °C.

The effect of the HAp precipitation on the specific surface area in the heat treatment was also evaluated. At first, the effect of HAp precipitation and acid treatment on the specific surface area was evaluated. The specific surface area of the sample after the HAp precipitation and acid treatment was measured and was 47 m^2/g. Since this value shows no significant difference with that of P25 (45 m^2/g), the steps of HAp precipitation and acid treatment is found to have little influence to the specific surface area of P25. Fig. 6 shows the changes of specific surface areas of the three-step and the one-step samples as a function of heating temperature. The on-set temperatures of decreasing of the specific surface area were clearly different between the two samples and about 100 °C higher in the three-step sample. This result indicates that the three-step procedure was effective to suppress decreasing of specific surface area as well as phase transformation to rutile in the heat treatment. It is considered that these effects are derived from the prevention of direct contact of the anatase particles (Fig. 4) as was reported in TiO_2–SiO_2 system [9].

3.3. Photocatalytic activities of the TiO_2 powders

The photocatalytic activities of the three-step samples were evaluated using a MB aqueous solution under UV irradiation (1.0 mW/cm^2). Fig. 7 shows the changes of MB concentration normalized by the initial concentration (C/C_0) as a function of UV irradiation time. The MB decomposition rate was the highest by heating at 700 °C. It is general that a photocatalytic

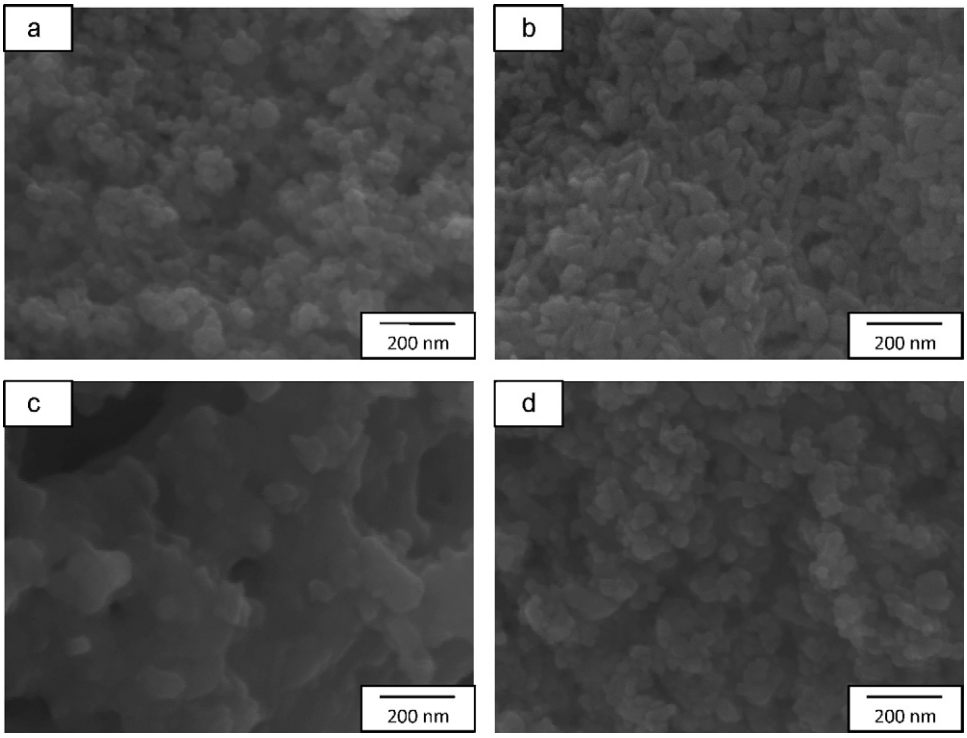

Fig. 4. SEM images obtained in a series of synthetic procedures (a) starting material, (b) after precipitation, (c) after heat treatment at 700 °C, and (d) after acid treatment.

activity shows a local maximum against heating temperature; this is due to a balance among recombination rate of electron–hole pairs, anatase phase ratio, and specific surface area.

All the data in Fig. 7 were well fitted by assuming first-order reaction represented by the following formula:

$$\ln\left(\frac{C_t}{C_0}\right) = -k_1 t, \tag{2}$$

where C_t and C_0 were the MB concentrations at time t and 0, respectively, and k_1 was the rate constant of first-order reaction (min^{-1}). The k_1 values of the three-step and one-step samples are shown in Fig. 8 as a function of heating temperature. The three-step samples had apparently higher rate constants than the one-step samples at all heating temperatures. For the samples without heating (R.T. samples), the k_1 of the three-step sample was about 1.1 times higher than the one-step sample (P25). This suggests that a moderate acid treatment has positive effect for photocatalytic activity of P25, e.g. improving dispersibility. The k_1 values increased by heat treatment and showed the maximum rate constant at 700 °C ($k_1 = 0.12$) in the three-step sample. The k_1 values of the one-step samples showed similar trend and showed the maximum at 650 °C ($k_1 = 0.08$). Thus, the

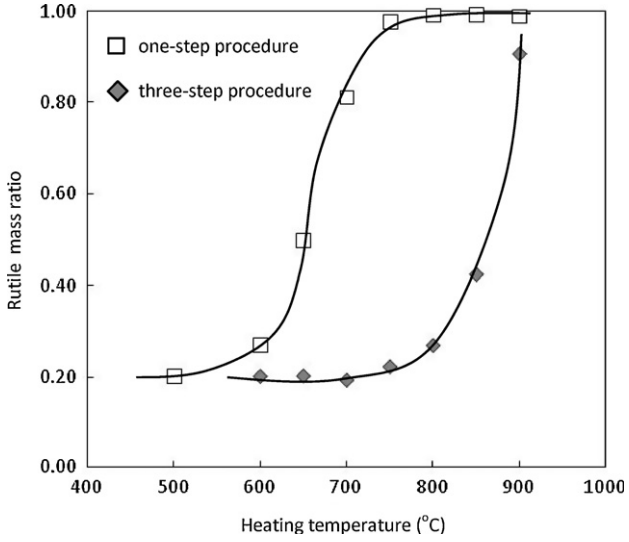

Fig. 5. Phase transformation curves from anatase to rutile obtained in three-step procedure and one-step conventional heating procedure.

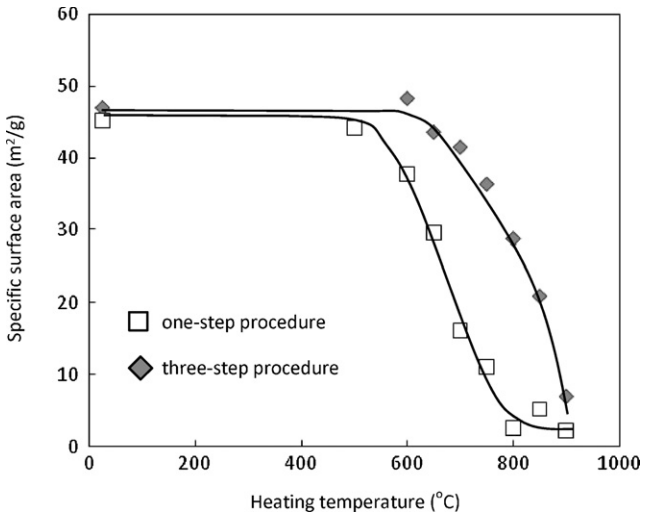

Fig. 6. Specific surface area measured by N_2-BET method obtained in three-step procedure and one-step conventional heating procedure.

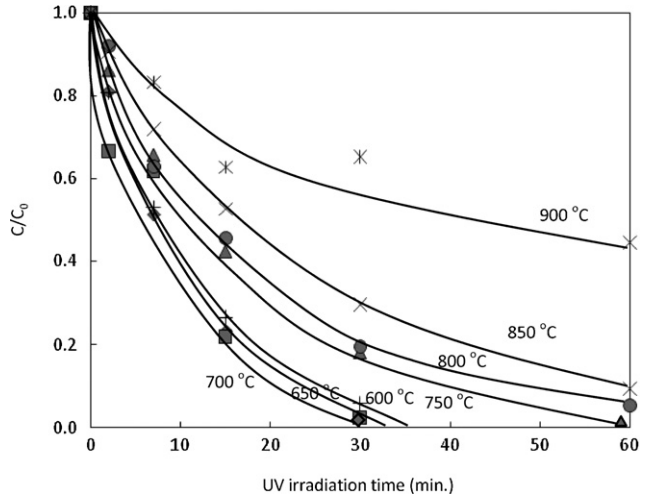

Fig. 7. Decrease curves of methylene blue concentration ratios (C/C_0) under UV irradiation with various heating temperatures in three-step procedure.

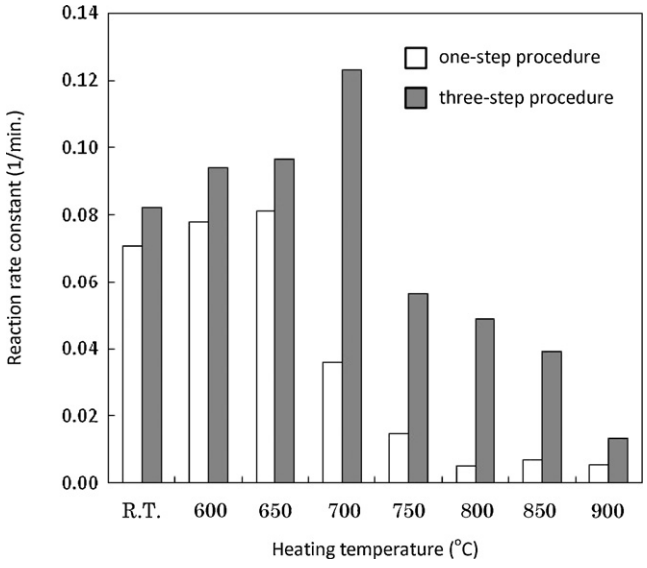

Fig. 8. Photocatalytic activity evaluated from decrease of methylene blue concentration obtained in three-step procedure and one-step conventional heating procedure.

maximum k_1 of the three-step sample was found to be 50 °C higher temperature. Although both samples showed a drastic decrease of the k_1 values above the maximum k_1 heating temperature, the k_1 values of the three-step samples were 1.5 times higher than that of the one-step samples.

From the above results, the following changes are thought to occur in the samples with higher heating temperatures: (1) clear decrease of specific surface area by coalescence of grains, (2) maximum decomposition rate as a trade-off relationship between higher calcination temperature and lower specific surface area, and (3) increase of anatase-to-rutile phase transformation by further increasing of grain size. The three-step procedure is considered to be effective to suppress the starting of drastic decrease of specific surface area about 100 °C compared with the conventional one-step procedure and this increment was very effective to enhance the photocatalytic activity without using hydrothermal conditions [21–23] and any organic solvents [24]. This three-step procedure is, thus, more suitable mass-production procedure for TiO_2 with high photocatalytic activity compared with other procedures.

4. Conclusion

TiO_2 powders were prepared by three-step procedure, precipitation of hydroxyapatite (HAp) on the TiO_2 particles (TiO_2/HAp composite), heat treatment at 600–900 °C, and acid treatment (obtaining of TiO_2 particles by removing of the HAp). The following results were obtained:

The three-step procedure was effective to suppress a loss of specific surface area and anatase-to-rutile phase transformation compared with that of the one-step procedure (conventional heating of P25 powders). This effect was considered to be achieved by avoiding of the direct contact of TiO_2 particles in the heat treatment.

The photocatalytic activities of the samples heated at various temperatures were clearly enhanced in the three-step samples compared with the one-step samples. The maximum MB photodecomposition rate constant was obtained by heating at 700 °C in the three-step sample and was about 1.5 times higher than that of the one-step sample (P25).

References

[1] K. Honda, A. Fujishima, Electrochemical photolysis of water at a semiconductor electrode, Nature 238 (1972) 37.
[2] T. Watanabe, T. Takizawa, K. Honda, Photocatalysis through excitation of adsorbates. 1. Highly efficient N-deethylation of rhodamine B adsorbed to Cds, J. Phys. Chem. 81 (19) (1977) 1845–1851.
[3] T. Kawai, T. Sakata, Conversion of carbohydrate into hydrogen fuel by a photocatalytic process, Nature 286 (1980) 474–476.
[4] H. Kominami, J. Kato, Y. Takada, Y. Doushi, B. Ohtani, S. Nishimoto, M. Inoue, T. Inui, Y. Kera, Novel synthesis of microcrystalline titanium (IV) oxide having high thermal stability and ultra-high photocatalytic activity: thermal decomposition of titanium (IV) alkoxide in organic solvents, Catal. Lett. 46 (1997) 235–240.
[5] B. Ohtani, R.M. Bowman, D.P. Colombo Jr., H. Kominami, H. Noguchi, K. Uosaki, Femtosecond diffuse reflectance spectroscopy of aqueous titanium oxide (IV) suspension: correlation of electron–hole recombination kinetics with photocatalytic activity, Chem. Lett. 1998 (1998) 579–580.
[6] M. Sakanoue, Y. Kinoshita, Y. Otsuka, H. Imai, Photocatalytic activities of rutile and anatase nanoparticles selectively prepared from an aqueous solution, J. Ceram. Soc. Japan 115 (2007) 821–825.
[7] D.J. Reidy, J.D. Holmes, M.A. Morris, Preparation of highly thermally stable titania anatase phase by addition of mixed zirconia and silica dopants, Ceram. Int. 32 (2006) 235–239.
[8] J. Zhang, M. Li, A. Feng, J. Chen, C. Li, UV Raman spectroscopic study on TiO_2. I. Phase transformation at the surface and in the bulk, J. Phys. Chem. B 110 (2006) 927–935.
[9] K. Okada, N. Yamamoto, Y. Kameshima, A. Yasumori, Effect of silica additive on the anatase-to-rutile phase transition, J. Am. Ceram. Soc. 84 (7) (2001) 1591–1596.
[10] M. Hirano, K. Ota, H. Iwata, Direct formation of anatase (TiO_2)/silica (SiO_2) composite nanoparticles with high phase stability of 1300 °C from acidic solution by hydrolysis under hydrothermal condition, Chem. Mater. 16 (2004) 3725–3732.
[11] X. Ding, L. Liu, X. Ma, Z. Qi, Y. He, The influence of alumina dopant on the structural transformation of gel-derived nanometer titania powders, J. Mater. Sci. Lett. 13 (1994) 462–464.

[12] H. Park, H.S. Jie, B. Neppolian, K. Tsujimaru, J.P. Ahn, D.Y. Lee, J.K. Park, M. Anpo, Preparation of highly active TiO_2 nano-particle photocatalysts by flame aerosol method for the complete oxidation of 2-Propanol, Top. Catal. 47 (2008) 166–174.

[13] Y. Sun, T. Egawa, L. Zhang, X. Yao, High anatase-rutile transformation temperature of anatase titania nanoparticles prepared by metalorganic chemical vapor deposition, Jpn. J. Appl. Phys. Pt. 2 41 (8B) (2002) 945–948.

[14] M. Inagaki, Y. Nakazawa, M. Hirano, Y. Kobayashi, M. Toyoda, Preparation of stable anatase-type TiO_2 and its photocatalytic performance, Int. J. Inorg. Mater. 3 (2001) 809–811.

[15] K.Y. Jung, S.B. Park, Anatase-phase titania: preparation by embedding silica and photocatalytic activity for the decomposition of trichloroethylene, J. Photochem. Photobiol. A: Chem. 127 (1999) 117–122.

[16] T. Nonami, H. Hase, K. Funakoshi, Apatite-coated titanium dioxide photocatalyst for air purification, Catal. Today 96 (2004) 113–118.

[17] T. Kokubo, H. Kim, M. Kawashita, Novel bioactive materials with different mechanical properties, Biomaterials 24 (2003) 2161–2175.

[18] J. Zhao, J. Liu, J. Wu, K. Tsuru, S. Hayakawa, A. Osaka, Apatite formation on rutile and anatase layers derived by hydrolysis of titanyl-sulfate in a simulated body fluid, J. Ceram. Soc. Japan 114 (3) (2006) 253–258.

[19] K. Okada, T. Yanagisawa, Y. Kameshima, A. Nakajima, Properties of TiO_2 prepared by acid treatment of $BaTiO_3$, Mater. Res. Bull. 42 (2007) 1921–1929.

[20] R.A. Spurr, H. Myers, Quantitative analysis of anatase–rutile mixtures with an X-ray diffractometer, Anal. Chem. 29 (1957) 760–762.

[21] J. Yu, H. Yu, B. Cheng, X. Zhao, Q. Zhang, Preparation and photocatalytic activity of mesoporous anatase TiO_2 nanofibers by a hydrothermal method, J. Photochem. Photobiol. A: Chem. 182 (2006) 121–127.

[22] K. Yamamoto, H. Shimoita, K. Tomita, K. Fujita, M. Kobayashi, V. Petrykin, M. Kakihana, Photocatalytic activity of nanocrystalline TiO_2(B) synthesized from titanium glycolate complex by hydrothermal method, J. Ceram. Soc. Japan 117 (3) (2009) 347–350.

[23] S. Yang, L. Gao, Preparation of titanium dioxide nanocrystallite with high photocatalytic activity, J. Am. Ceram. Soc. 88 (4) (2005) 968–970.

[24] H. Kominami, J. Kato, S. Murakami, M. Kohno, Y. Kera, S. Nishimoto, M. Inoue, T. Inui, B. Ohtani, Thermal treatment of titanium alkoxides in organic media: novel synthesis methods for titanium (IV) oxide photocatalyst of ultra-high activity, Stud. Surf. Sci. Catal. 130 (2000) 1937–1943.